

Temperature dependence of the quadrupole interaction for ^{100}Rh , ^{111}Cd , and ^{181}Ta in Be

K. Krien, J. C. Soares,* K. Freitag, R. Tischler, G. N. Rao, and H. G. Müller
Institut für Strahlen- und Kernphysik der Universität Bonn, Germany

E. N. Kaufmann
Bell Laboratories, Murray Hill, New Jersey 07974

A. Hanser and B. Feurer
Gesellschaft für Kernforschung GmbH, Karlsruhe, Germany
 (Received 8 April 1976)

The temperature dependence of the electric field gradients at ^{100}Rh , ^{111}Cd , and ^{181}Ta impurities in Be have been measured by time-differential perturbed-angular-correlation methods. The observed temperature dependences are quite different. The interaction frequencies decrease for ^{100}Rh and ^{111}Cd with rising temperature, but increase for ^{181}Ta , which is quite unusual. The probes were produced by ion implantation of the activities ^{100}Pd , ^{111}In , and ^{181}Hf . Channeling experiments showed that Pd implanted into Be occupies substitutional sites. The results are compared with presently discussed models.

I. INTRODUCTION

Systematic investigations of the temperature dependence of electric field gradients (EFG) at sites of impurities in metals revealed recently new interesting phenomena: Whereas the EFG temperature dependences of a number of impurities in the hosts Cd (Ref. 1) and Zn (Ref. 2) were found to be very similar to those of the pure metals, the Ti host shows the opposite effect. At ^{181}Ta , ^{111}Cd , and ^{44}Sc impurity sites^{3,4} in Ti quite different temperature dependences were observed. This different behavior is not yet understood and more systematic studies are needed.

Be metal is a particularly attractive host. It belongs to the same group of the periodic system as Cd and Zn, but it has a much simpler electronic configuration, namely only four *s* electrons. Conduction-electron wave functions for this metal are quite well known⁵ and *ab initio* calculations⁶ of the effective EFG at the Be site in the pure matrix exist, which are in agreement with experiment.⁷

Recently room-temperature time-differential perturbed-angular-correlation (TDPAC) experiments⁸ with the 84-nsec 247-keV state of ^{111}Cd in Be yielded an electric quadrupole coupling constant $\nu_q = -17$ MHz, when the ^{111}Ag parent radioactivity was implanted but $|\nu_q| = 54$ MHz when $^{111}\text{Cd}^m$ or ^{111}In were used. Channeling experiments⁸ proved that only Ag occupies substitutional sites in Be, whereas Cd and In are interstitial. Similar experiments⁹ with ^{181}Ta in Be (from ^{181}Hf implantation) showed that ^{181}Ta is also at a tetrahedral interstitial site and exhibits an unique quadrupole interaction (QI). From the standpoint of the presently discussed theories for EFG tem-

perature dependences, it is especially attractive to see if substitutional and interstitial sites behave differently.

In this paper we report measurements of the temperature dependence of the EFG's at ^{100}Rh , ^{111}Cd , and ^{181}Ta in Be metal. In order to facilitate the interpretation of the Be ^{100}Rh data, the lattice location of Pd in Be was determined by channeling experiments.

II. TDPAC EXPERIMENTS AND RESULTS

A. Experimental procedures

For our measurements of the QI frequencies, TDPAC methods were used. The radioactivities were implanted into Be foils using electromagnetic isotope separators of 70–80-kV accelerating potentials. The 150- μm Be foils were cleaned mechanically before the implantations. After implantation they were cleaned with methanol. Only for the γ - γ experiment was the Be foil broken into small pieces, which were filled into a 3-mm-diam Al sample holder. The relevant information concerning source production methods and properties of the nuclear decays are given in Table I for all three isotopes.

The conversion-electron- γ TDPAC measurements were performed with magnetic lens β spectrometers and a movable NaI(Tl) γ detector. For the γ - γ TDPAC experiment, a conventional angular correlation apparatus was used. In all experiments the angles between detectors were changed every 1000 sec and time spectra at 180° and 90° were stored in separate subgroups of multichannel analyzers. A detailed description of the e^- - γ angular correlation apparatus is given in Ref. 10. For more information about the source produc-

TABLE I. Sample production data and nuclear decay properties.

Nuclide studied	¹⁰⁰ Rh	¹¹¹ Cd	¹⁸¹ Ta
Parent activity	¹⁰⁰ Pd	¹¹¹ In	¹⁸¹ Hf
Production method	¹⁰³ Rh(50-Mev <i>d</i> , 5 <i>n</i>) ¹⁰⁰ Pd	Purchased from New England Nuclear Corp.	Natural Hf oxide (<i>n</i> , γ) ¹⁸¹ Hf
Total dose of im- planted ions per cm ²	$< 5 \times 10^{14}$	$< 2 \times 10^{14}$	$\left\{ \begin{array}{l} \sim 0.5 \times 10^{14} \text{ Hf}^a \\ \sim 3 \times 10^{14} \text{ W} \end{array} \right.$
Cascade radiation	84-keV γ - 75-keV $K e^-$	173-keV γ - 247-keV γ	133-keV $K e^-$ - 482-keV γ
Intermediate level:			
Half-life $T_{1/2}$ (nsec)	215	84	10.6
Spin and parity	2 ⁺	$\frac{5}{2}^+$	$\frac{5}{2}^+$

^a Chlorination technique, W dose from ion-source filament.

tion of the ¹⁰⁰Pd sample, see Ref. 11 which refers to a similar experiment in a Zn lattice. The ¹⁸¹Ta experiment was similar to the determination of QI for ¹⁸¹Ta in a Be single crystal at room temperature reported earlier.⁹

For measurements below room temperature, the radioactive samples were attached to cooling fingers of appropriate cryostats filled with liquid He, liquid N₂, or refrigerated methanol depending on the desired temperature. For measurements above 293 °K, the samples were fixed at the tips of electrically heated copper rods or, in the case of ¹¹¹Cd in Be, immersed in a heated oil bath. The temperatures of the samples were monitored by thermocouples. The thermopotentials were also used to regulate the power input to the heating devices. Owing to calibration uncertainties we estimate the quoted temperatures may be up to $\pm 5^\circ$ in error.

B. TDPAC results

The results of the TDPAC measurements at room temperature are plotted in Figs. 1–3(a) for

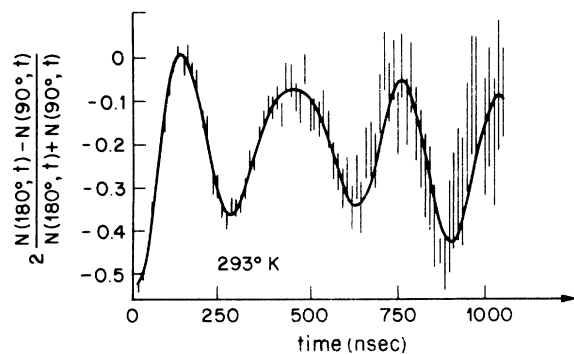


FIG. 1. Quadrupole precession curve for ¹⁰⁰Rh in Be at room temperature.

¹⁰⁰Rh, ¹¹¹Cd, and ¹⁸¹Ta, respectively, where the asymmetry ratios

$$R(t) = 2 \frac{N(180^\circ, t) - N(90^\circ, t)}{N(180^\circ, t) + N(90^\circ, t)}$$

are plotted versus the delay time. $N(180^\circ, t)$ and $N(90^\circ, t)$ are the time spectra obtained with angles of 180° and 90° between the detectors. For ¹⁰⁰Rh and ¹¹¹Cd at all temperatures similar patterns were observed, displaying unique quadrupole rotations with only very small frequency distributions being indicated for ¹⁰⁰Rh.

For ¹⁸¹Ta in the previous single-crystal experiment⁹ similar small frequency distributions had been observed without further treatments of the sample. In the present experiment an almost complete destruction of the rotational pattern was encountered [Fig. 3(a)]. In a second experiment at 468 °K (Fig. 4) the expected rotational pattern appeared, implying that an annealing process had occurred. On measuring at room temperature again [Fig. 3(b)], the unique QI remained. Further measurements were performed at 379, 215, 559, 624, and 657 °K (Fig. 4). The amplitude of the spin rotation pattern decreases at the two highest temperatures. A final experiment at room temperature showed that an irreversible change of the

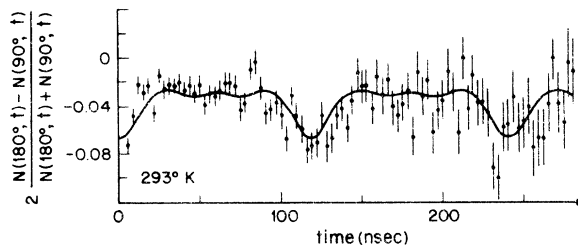


FIG. 2. Quadrupole precession curve for ¹¹¹Cd in Be at room temperature.

sample had taken place [Fig. 3(c)] at the highest temperatures.

All measured asymmetry ratios $R(t)$ could be least-squares fitted to the function

$$R(t) \approx \frac{3}{2} A_2 b_2 \left(f \sum_n S_{2n} \cos n \omega_0 t e^{-(n^6 \omega_0 t)^2 / 2} + (1-f) \sum_n S_{2n} \cos n \omega'_0 t e^{-(n^6 \omega'_0 t)^2 / 2} \right).$$

Nonzero, but small terms involving the A_4 coefficient for ^{181}Ta have been neglected. For the γ - γ TDPAC experiment with ^{111}Cd the conversion-electron-particle parameter b_2 is to be set equal to one. The index n and parameters S_{2n} take values determined by the spin of the intermediate level of the cascade. The first term of this theoretical function accounts for quadrupole precessions of nuclei in the axially symmetric EFG in the Be lattice, which is usually associated with a unique site. The multiplicative exponential factors allow for slight frequency distributions mainly due

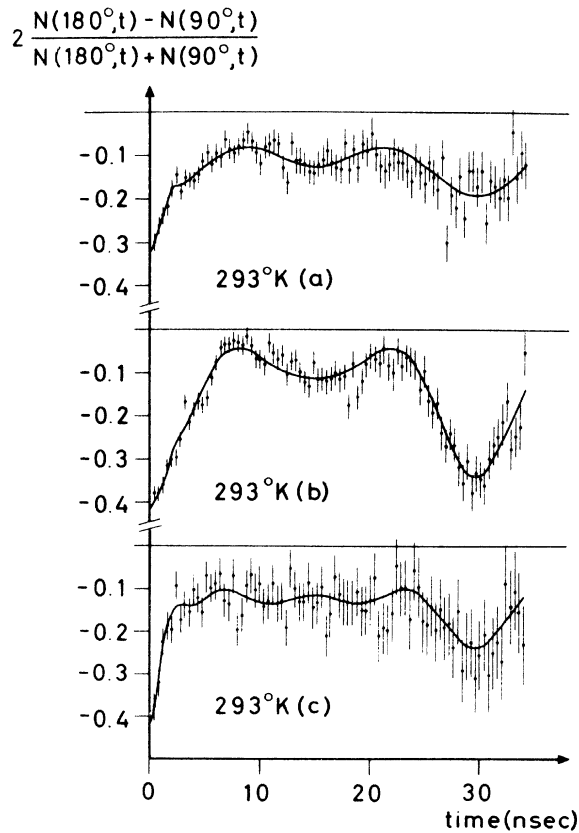


FIG. 3. Quadrupole precession curves for ^{181}Ta in Be at room temperature. (a) directly after implantation; (b) after measurement at 468 °K; (c) after measurement at 657 °K.

to radiation-damage effects. The second term is added to account for the fraction $1-f$ of nuclei in irregular lattice positions, where a large spread in QI strength of assumed Gaussian shape with relative width δ' around a mean QI frequency ω'_0 exists.

For ^{100}Rh , data were fitted well for a fixed value of $f=1$ and δ was found to be extremely small; $\delta=0.03(1)$. For the ^{111}Cd and ^{181}Ta data, δ could be kept fixed at zero, since no decrease of the unique frequency amplitudes is observed. In addition, for ^{111}Cd δ' must be extremely large since the second term of the theoretical perturbation function could well be approximated by a constant. For the data of ^{100}Rh and ^{181}Ta taken with an unbroken Be foil, the parameters S_{2n} were fitted in preliminary computations in order to allow for possible partial alignments of the microcrystals

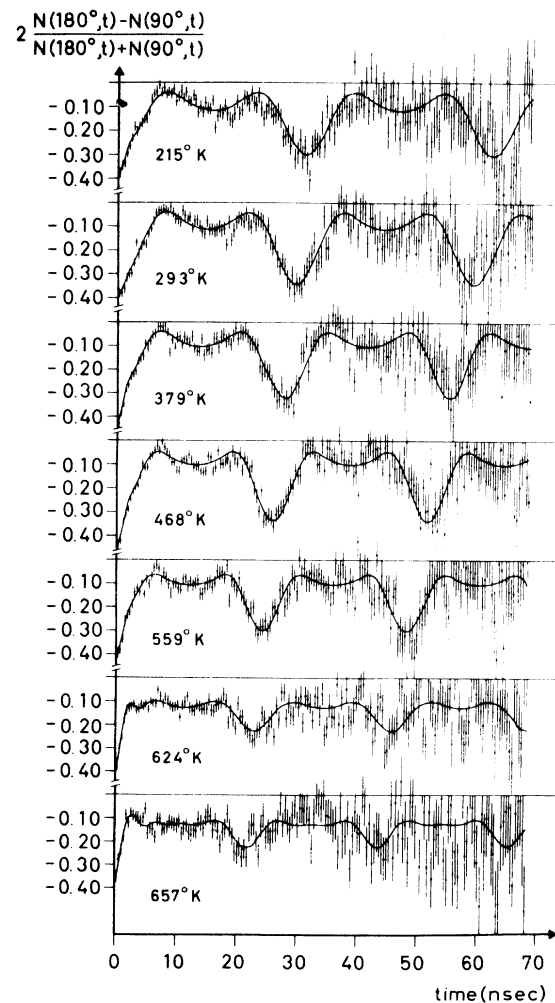


FIG. 4. Quadrupole precession curves for ^{181}Ta in Be at various temperatures.

of the Be foil. In the final analysis they were kept fixed at averaged values, which were very close to those theoretically expected¹² for the respective spin of the intermediate level and a polycrystalline Be foil.

The fitted parameters A_2b_2 agree with the conversion-electron-particle parameter and angular correlation predictions for ^{100}Rh and ^{181}Ta after corrections for scattering and finite solid angles are taken into account. This may not seem to be true according to Figs. 3 and 4 for ^{181}Ta , but the apparent smaller effective anisotropy for some measurements are due to finite-time-resolution effects, affecting particularly strongly the fast frequencies at the nonunique sites. These effects are taken into account in the fitting procedures. The low A_2 coefficients for our ^{111}Cd experiments are in agreement with a previous experiment with the same system.⁸ The fraction of atoms observed at unique sites has been seen to be smaller when polycrystalline foils are used¹³ as opposed to single-crystal⁸ samples. This is also consistent with our low-anisotropy results.

The solid lines in Figs. 1–4 are the result of the described fitting procedures. The experimental QI coupling constants

$$\nu_q = eQV_{zz}/\hbar$$

for ^{100}Rh , ^{111}Cd , and ^{181}Ta are given in Tables II–IV, respectively. Since for ^{181}Ta , the parameters ν'_q , δ' , and f are temperature dependent, they have been summarized in Table IV as well. The derived quadrupole coupling constants at 293 °K are in agreement with previous experimental results with the same systems.^{8,9,13} This is in particular true for all three room-temperature experiments (runs 1, 3, 9 of Table IV) with ^{181}Ta . We must therefore assume that the fraction of nuclei contributing to the unique frequencies is at the same interstitial site as determined by the channeling experiment.⁹ The reason for the very low unique site occupation probability $f=0.13$ observed in the first run compared to $f=0.84$ for the single-crystal experiment⁹ is not clear. It

TABLE II. Quadrupole coupling constants $\nu_q = eQV_{zz}/\hbar$ for ^{100}Rh in metallic Be. Errors given as uncertainties in the last significant digits include time calibration uncertainties.

T (°K)	ν_q (MHz)
106	9.03(10)
198	8.97(10)
293	8.86(10)
394	8.66(10)
513	8.35(10)

TABLE III. Quadrupole coupling constants $\nu_q = eQV_{zz}/\hbar$ for ^{111}Cd in Be. Errors given as uncertainties in the last significant digits include time calibration uncertainties.

T (°K)	ν_q (MHz)
23	58.8(7)
79	58.0(7)
293	55.3(10)
431	52.9(6)

may be due to a number of circumstances, e.g., (i) more radiation damage due to the difficulties with this particular implantation, (ii) effects due to the additionally implanted W, (iii) lower purity of the host lattice and higher density of grain boundaries than in a single crystal. When the foil was heated to 468 °K annealing occurred, which was, however, not complete. The unique site occupation probability increased to $f=0.4$. Furthermore, the mean nonunique coupling constant ν'_q dropped from 2370 to 1660 MHz and the width of the frequency distribution dropped from $\delta'=0.81(15)$ to $\delta'=0.55(15)$. The sample did not change its properties thereafter at any temperature up to 559 °K, since f and δ' remained constant within errors and ν'_q seems to decrease in a continuous manner with rising temperature irrespective of the temperature of the sample in the previous run. Above 600 °K the unique site occupation probability dropped to $f=0.18$. At the same time δ' decreased further to $\delta'\approx 0.4$. These values remained unchanged in the last run (No. 9) at room temperature and the frequency ν'_q remained as in the high-temperature experiment. It is tempting to associate this second change at 600 °K with a migration of the originally interstitial Hf ions to grain boundaries where precipitation occurs, but more evidence is needed before this can be definitely concluded.

TABLE IV. Quadrupole coupling constants (ν_q) and unique site occupation probabilities (f) for ^{181}Ta in Be at different temperatures.

Run	T (°K)	ν_q (MHz)	ν'_q (MHz)	δ'	f
5	215	217.7(3.5)	1820(36)	0.55(15)	0.36(5)
1	293	234.2(5.8)	2370(46)	0.81(15)	0.13(2)
3	293	228.9(3.4)	1750(35)	0.55(15)	0.40(2)
9	293	231.6(4.2)	1403(30)	0.38(15)	0.19(3)
4	379	248.6(3.6)	1700(35)	0.55(15)	0.36(4)
2	468	261.1(3.7)	1660(32)	0.55(15)	0.39(4)
6	559	278.2(4.1)	1550(30)	0.55(15)	0.39(4)
7	624	293.9(5.3)	1480(30)	0.40(10)	0.17(2)
8	657	308.9(6.5)	1340(30)	0.30(10)	0.18(3)

III. LATTICE LOCATION STUDIES OF Pd IN Be

The lattice location of implanted Pd in Be was studied using ion beam channeling of 1.9-MeV He^+ ions. The same Be single crystal as was used for the previous Hf in Be channeling experiment⁹ was employed after previously implanted impurities had been removed by mechanical polishing and chemical etching. A dose of 2.5×10^{14} ions/cm² of ^{105}Pd were implanted at an energy of 100 keV. The sample was held at room temperature and oriented to avoid channeling of the implanted ions. The Pd ions were produced by use of a Hill-Nelson sputtering ion source associated with the Bell Laboratories isotope separator. Two single-channel analyzers selected He^+ ions Rutherford scattered from the Be host and the Pd impurity, respectively. Using techniques identical to those described in Ref. 9, relative scattering yields were measured as a function of the angle made by the incident beam to a channeling direction of the crystal. The (0001) planar channel (basal plane) and the $\langle 11\bar{2}0 \rangle$ axial channel (\hat{a} axis) were studied. The yields corresponding to He scattered from the Be host and Pd impurity are displayed in Figs. 5 and 6, where the average yield is normalized to unity for angles off the channeling direction. Any nonsubstitutional component would evidence itself as a difference in the angular dependence of the scattered flux from the Pd impurity as opposed to the Be host. The identical results for scattering from host and impurity along both channels studied reveals that virtually all of the implanted Pd atoms occupy substitutional sites and that they

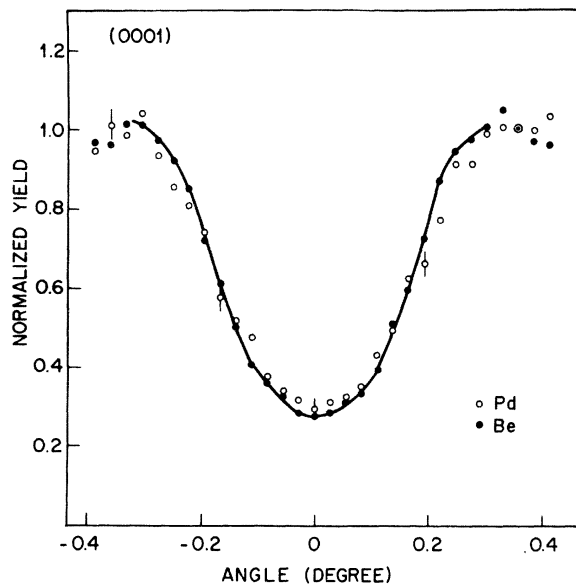


FIG. 5. Angular scan of the (0001) plane. Curve is drawn to guide the eye.

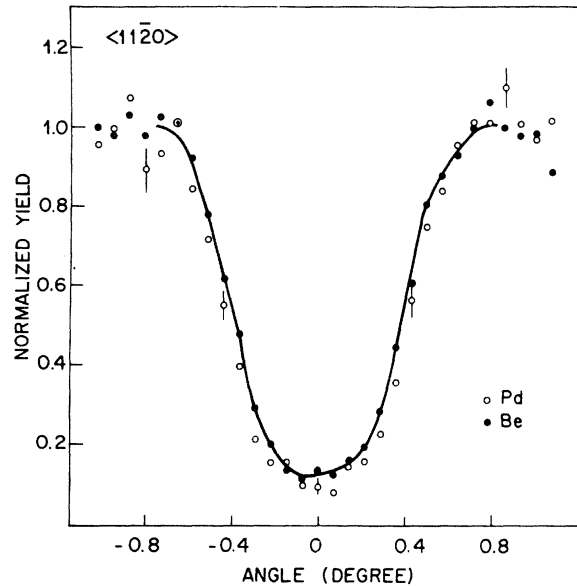


FIG. 6. Same as Fig. 5 for $\langle 11\bar{2}0 \rangle$ axis. Curve is drawn to guide the eye.

are not closely coordinated with lattice defects. This result agrees with the conclusion of Ref. 14 where TDPAC spectra indicated that practically all of the implanted Pd radioisotope was on the same unique site in Be. The result is also consistent with the observation⁸ that impurities having at least limited solid solubility in Be, as Pd does,¹⁵ will tend to prefer regular lattice sites after implantation.

IV. TEMPERATURE DEPENDENCES OF THE UNIQUE QI FREQUENCIES IN Be

The EFG's for ^9Be , ^{100}Rh , ^{111}Cd , and ^{181}Ta in Be at room temperature have been discussed before (Refs. 7-9 and 14). We therefore restrict the discussion to the temperature dependence. The QI temperature dependence for the five probes ^9Be , ^{57}Fe , ^{100}Rh , ^{111}Cd , and ^{181}Ta in Be metal is plotted in Fig. 7, where the data are normalized to unity at room temperature to eliminate uncertainties of the quadrupole moments of the probe nuclei. The data for ^9Be and ^{57}Fe are taken from Refs. 7 and 16, respectively. The changes of the effective EFG's with temperature are quite different for the various probes. In particular the magnitude of the EFG for ^{181}Ta in Be increases with rising temperature. This behavior is opposite to all previous experiments with small impurity concentrations in elemental metallic hosts. The only exceptions known to the authors are systems involving impurities in intermetallic compounds (e.g., Ref. 17).

In order to compare observed temperature dependences with point-charge-model predictions, we have calculated the lattice and ionic EFG's in Be for the impurities of interest (see Table V). The ionic EFG defined as in Ref. 18, i.e., the sum of the point-charge part of the EFG and the contribution by the closed shells of the impurity can be calculated by multiplication of the lattice EFG with the appropriate Sternheimer antishielding factor: $V_{zz}^{\text{ion}}(\text{impurity}) = V_{zz}^{\text{lat}}[1 - \gamma_{\infty}(\text{impurity})]$. For the computation of the point-charge lattice contribution the formula of Das and Pomerantz¹⁹ is not applicable to the case of interstitial sites. Therefore, we followed a spherical summation procedure by Ewald²⁰ using an ionic charge of $+2e$. The lattice constants were taken from Ref. 21. Unfortunately for temperatures below 293°K, exact lattice constants are apparently not available. The Sternheimer antishielding factors,²² $1 - \gamma_{\infty} = 0.8144$, 30.3, and 62 were used for Be, Cd, and Ta, respectively. The value $1 - \gamma_{\infty} = 19$ for Rh was taken from the tables of Ref. 23. Since ¹¹¹Cd and ¹⁸¹Ta are on tetrahedral sites with lattice coordinates $(\frac{2}{3}, \frac{1}{3}, y)$ where the displacement y of the impurity from the (0001) basal plane could not be determined exactly from the channeling data,^{8,9}

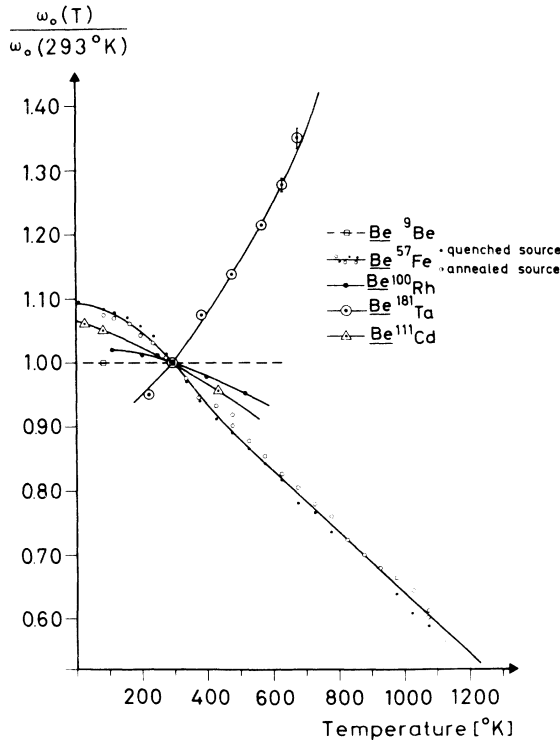


FIG. 7. QI temperature dependences for various impurities in Be. The data are normalized to unity at room temperature.

TABLE V. Parameters for EFG contributions. For explanations of parameter y see text.

T (°K)	293	473	673	873	1273
c/a	1.5677	1.5670	1.5658	1.5646	1.5620
a (Å)	2.2854	2.292	2.300	2.309	2.330
V_{zz}^{lat} (substitutional) (10^{16} V/cm ²)	0.7084	0.7097	0.7146	0.7185	0.7249
$V_{zz}^{\text{ion}} = (1 - \gamma_{\infty})V_{zz}^{\text{lat}}$ (10^{17} V/cm ²)					
Be (sub)	0.0577	0.0578	0.0582	0.0585	0.0590
Rh (sub)	1.346	1.348	1.358	1.366	1.377
V_{zz}^{lat} (tetrahedral) (10^{16} V/cm ²)					
$y = 0.110$	-2.011	-1.967	-1.902	-1.836	-1.692
$y = 0.120$	+1.276	+1.292	+1.325	+1.355	+1.416
$y = 0.125$	+3.004	+3.006	+3.022	+3.034	+3.052
$y = 0.130$	+4.790	+4.776	+4.775	+4.768	+4.742
y for middle tetrahedral site	0.11437	0.11425	0.11404	0.11383	0.11338
V_{zz}^{ion} (middle y) (10^{17} V/cm ²)					
¹¹¹ Cd	-1.82	-1.85	-1.89	-1.94	-2.02
¹⁸¹ Ta	-3.74	-3.78	-3.88	-3.97	-4.13

we have calculated the lattice and ionic EFG's for several values of the parameter y .

A. Substitutional impurities

1. ¹⁰⁰Rh

The interpretation of the observed QI temperature dependence for ¹⁰⁰Rh in Be is difficult because the quadrupole moment of the 75-keV state is unknown and not even an absolute value of the effective EFG can be deduced. The magnitude of the observed QI coupling constant decreases with rising temperatures. This is a quite usual behavior for impurities in metallic lattices²⁴ (see, e.g., the recent compilation of measured QI frequencies). Electronic EFG contributions at the substitutional site in Be can be quite large. For substitutional Cd in Be it has been shown,⁸ by a $\beta - \gamma$ TDPAC measurement using ¹¹¹Ag as radioactive parent, that these contributions are of opposite sign to the lattice field and about three times larger. The experimental ¹⁰⁰Rh QI temperature dependence has an opposite slope than the calculated ionic EFG at the substitutional site, which increases slightly with temperature. This result is similar to observations for Rh in Zn,¹¹ and Cd,¹ where such discrepancies have been interpreted in terms of temperature dependent electronic contributions. Quitmann²⁵ and Jena²⁶ have pointed out that thermal lattice vibrations may be an important contributing mechanism in this temperature dependence.

2. ^9Be

For Be in Be the QI is approximately temperature independent. Since in pure-Be metal with only four s electrons no large electronic EFG's should be present, the EFG should be determined essentially by the lattice part, which does not change much with temperature. This expectation is supported by theoretical calculations⁶ which ascribe the observed EFG for Be mainly to ionic contributions. Electronic contributions from different energy bands essentially cancel each other. The consistency of the Be in Be QI data with the calculated ionic EFG and its temperature dependence indicates that lattice vibrational effects are less important in this pure case, possibly because of the unusually high Debye temperature of Be. If lattice vibrations are operative for the impurity case of Rh in Be, our results must therefore be interpreted in terms of a local vibrational mode at the heavy Rh atom site.

B. Interstitial impurities

1. ^{181}Ta

In order to discuss the EFG temperature dependence of the tetrahedral interstitial impurities, ^{111}Cd and ^{181}Ta , the value of the displacement y must be known because the lattice part of the EFG depends very sensitively on it. It even changes sign at $y \approx 0.166$ (Table V). This parameter cannot be determined by channeling experiments with sufficient accuracy. A reasonable assumption may be that the impurity takes a site equally distant from all four nearest neighbors of the host lattice. In an ideal hexagonal lattice with $c/a = (\frac{2}{3})^{1/2}$, $y = \frac{1}{8}$ satisfies this condition. In Be with $c/a = 1.5677$ the same assumption gives $y = \frac{1}{4} - a^2/3c^2 = 0.11437$ at room temperature and slightly lower values at higher temperatures (Table V). This value is consistent with the channeling data⁹ for Hf in Be, where $y = 0.110$ is in slightly better agreement with experiment than, e.g., $y = \frac{1}{8}$. For room temperature the calculated magnitude of the ionic EFG for ^{181}Ta at this middle tetrahedral site is very close to the experimental EFG⁹ $V_{zz}^{\text{exp}}(\text{Ta}) = \pm 3.71 \times 10^{17} \text{ V/cm}^2$. Therefore Ta in Be may be a case where the effective EFG is dominated by the ionic EFG and electronic contributions are very small. This result would not be surprising if the following assumptions are correct: Since at the tetrahedral site in Be there is not much space to accommodate an impurity with large ionic radius, a higher ionization state may be energetically favorable implying that the three $5d$ electrons of the Ta impurity go into the conduction band of the Be lattice and do not contribute significantly to the

electronic EFG acquiring essentially s character.

The predicted ionic EFG at the middle tetrahedral site increases with temperature. Experimentally a similar increase of the effective EFG is observed. However, since the experimental EFG increases more rapidly than the calculated ionic EFG, additional physical effects must be present. These could be due to lattice vibrations or changes in angular momentum state with temperature of the charge screening electrons. It is, however, perhaps most probable that the parameter γ varies with temperature in a different way than inferred above from purely geometrical considerations, since, e.g., preferred Be-Ta electron bonds or preferential lattice relaxations due to the size mismatch between Ta and Be are conceivable.

The above discussion assumes the sign of the EFG at Ta in Be is negative. If it were positive, to account for the measured effective EFG temperature dependence, an electronic contribution of twice the magnitude of the ionic EFG with opposite sign, which increases strongly with temperature in order to overcompensate the temperature dependence of the ionic EFG, would have to be assumed. We prefer the first interpretation, but a decision can only be obtained by a measurement of the sign of the QI for Ta in Be. Such a measurement by use of the Mössbauer effect with the 6-keV state in ^{181}Ta appears feasible.

2. ^{111}Cd

The impurity ^{111}Cd in Be, which is also at a tetrahedral interstitial site, exhibits a quite different temperature dependence than ^{181}Ta in Be. The effective EFG decreases slightly with rising temperature as is normally found for impurities in metallic hosts.²⁴ If ^{111}Cd and ^{181}Ta occupy identical tetrahedral sites in Be, this different behavior could be attributed to electronic contributions. Such electronic contributions are indicated in the Cd case since the ionic EFG calculated at the middle tetrahedral site for Cd in Be at room temperature is less in absolute value than the experimental EFG at the tetrahedral site,⁸ $V_{zz}^{\text{exp}}(\text{Cd in Be interstitial}) = -2.90 \times 10^{17} \text{ V/cm}^2$. The sign of the QI for Cd on the interstitial site has not been measured directly. An indirect inference as to the sign of the EFG at Cd in Be can be drawn from a sign measurement⁸ on ^{115}In , by β - γ PAC, with In at the tetrahedral site in Be. The EFG is negative at In. Assuming In and Cd to occupy identical sites in Be and further that the other EFG contributions are not very different for Cd and In, the effective EFG at Cd should also be negative. From this it follows that the electronic contributions should have the same sign as the

ionic part, are small and if responsible for the EFG temperature dependence decrease rapidly with rising temperatures in order to overcompensate the increase of the ionic EFG. However, it is equally well conceivable that any other mechanism mentioned above in context with BeTa EFG temperature dependence are important in the Cd case as well.

The authors of Ref. 8 gave a different interpretation of the field gradient for Cd in Be. They compare the ratio of the lattice EFG for the substitutional and interstitial sites with the ratio of the experimental QI coupling constants. Then with the assumption that the electronic contributions to the EFG are described in both cases by the same multiplicative factors, the lattice coordinates ($\frac{2}{3}, \frac{1}{2}, \gamma = 0.123$) for the position of the interstitial Cd ion are deduced. This value of γ is close to that expected for the ideal hexagonal lattice. The existing channeling data⁸ do not allow us to distinguish between these two interpretations.

Our discussion depends entirely on the assumption that the ¹¹¹Cd and ¹⁸¹Ta impurities occupy the middle tetrahedral site in Be. This idea is supported by the well-known fact that rather strong repulsive forces act if two ions approach each other closer than a critical distance. Considering the ionic radii of ¹⁸¹Ta and ¹¹¹Cd and the space available between the Be ions of the tetrahedron, we believe that the impurities are closer to the Be ions than this critical distance. We do, however, neglect effects such as preferred electronic

bonds or directionally dependent lattice relaxation, which may be important because the deviation of the c/a ratio of Be from its ideal value may imply that the four Be ions at the vertices of the tetrahedron are inequivalent. Some more insight into the way in which the value of the γ coordinate is determined is needed to clarify these issues.

Note added in proof. The recent appearance of a paper by K. Nishiyama, F. Dimmling, Th. Kornrumpf, and D. Riegel [Phys. Rev. Lett. **37**, 357 (1976)] strongly supports the notion that thermal lattice vibrations dominate the EFG temperature dependence in nontransition metals. This lends more credence to the suggestion of a local vibrational mode for the Be ¹⁰⁰Rh case.

ACKNOWLEDGMENTS

One of us (K.K.) would like to thank Bell Laboratories for their hospitality during the channeling experiments. The continuous interest in our work by Professor E. Bodenstedt is gratefully acknowledged. Thanks are due to J. W. Rodgers, W. F. Flood, W. M. Augustyniak, R. A. Boie, and M. F. Robbins for their assistance with the channeling experiment, as well as to Ch. Heising, F. J. Kappes, and W. Schaub for their assistance with the radioactive isotope separator implantations. Work performed in Germany was in part financially supported by the Minister für Wissenschaft and Forschung des Landes Nordrhein-Westfalen.

*On leave from the University of Lisbon, with a fellowship from the Instituto de Alta Cultura of Portugal.

¹K. Krien, J. C. Soares, R. Vianden, A. G. Bibiloni, and A. Hanser, *Hyp. Interact.* **1**, 295 (1975).

²K. Krien, J. C. Soares, K. Freitag, R. Vianden, and A. G. Bibiloni, *Hyp. Interact.* **1**, 217 (1975).

³E. N. Kaufmann, P. Raghavan, R. S. Raghavan, K. Krien, and R. A. Naumann, *Phys. Status Solidi B* **63**, 719 (1974); **75**, 803E (1975).

⁴R. C. Reno, R. L. Rasera, and G. Schmidt, *Phys. Lett. A* **50**, 243 (1974).

⁵T. P. Das, *Phys. Scr.* **11**, 121 (1975), and references therein.

⁶N. C. Mohapatra, C. M. Singal, T. P. Das, and P. Jena, *Phys. Rev. Lett.* **29**, 456 (1972).

⁷D. E. Barnaal, R. G. Barnes, B. R. McCart, L. W. Mohn, and D. R. Torgeson, *Phys. Rev.* **157**, 510 (1967).

⁸E. N. Kaufmann, P. Raghavan, R. S. Raghavan, E. J. Ansaldo, and R. A. Naumann, *Phys. Rev. Lett.* **34**, 1558 (1975).

⁹E. N. Kaufmann, K. Krien, J. C. Soares, and K. Freitag, *Hyp. Interact.* **1**, 485 (1976).

¹⁰K. Krien, A. G. Bibiloni, K. Freitag, J. C. Soares,

and R. Vianden, *Phys. Rev. B* **8**, 2248 (1973).

¹¹K. Krien, J. C. Soares, A. G. Bibiloni, R. Vianden, and A. Hanser, *Z. Phys.* **266**, 195 (1974).

¹²H. Frauenfelder and R. M. Steffen, in *Alpha-, Beta-, and Gamma-Ray Spectroscopy*, edited by K. Siegbahn (North-Holland, Amsterdam, 1966).

¹³E. N. Kaufmann, P. Raghavan, R. S. Raghavan, K. Krien, E. J. Ansaldo, and R. A. Naumann, in *Applications of Ion Beams to Metals*, edited by S. T. Picraux, E. P. EerNisse, and F. L. Vook (Plenum, New York, 1974), p. 379.

¹⁴K. Krien, J. C. Soares, A. Hanser, and B. Feurer, *Hyp. Interact.* **1**, 41 (1975).

¹⁵M. Hansen, *Constitution of Binary Alloys* (McGraw-Hill, New York, 1958), p. 293.

¹⁶C. Janot, P. Delcroix, and M. Piecuch, *Phys. Rev. B* **10**, 2661 (1974).

¹⁷H. Haas and D. A. Shirley, *J. Chem. Phys.* **58**, 3339 (1973).

¹⁸R. S. Raghavan, E. N. Kaufmann, and P. Raghavan, *Phys. Rev. Lett.* **34**, 1280 (1975); and P. Raghavan, E. N. Kaufmann, R. S. Raghavan, E. J. Ansaldo, and R. A. Naumann, *Phys. Rev. B* **13**, 2835 (1976).

¹⁹T. P. Das and M. Pomerantz, *Phys. Rev.* **123**, 2070

- (1961).
- ²⁰P. P. Ewald, *Ann. Phys. (Leipz.)* 64, 253 (1921); see also F. W. de Wette and G. E. Schacher, *Phys. Rev.* 137, A78 (1965); 137, A92 (1965), and references therein.
- ²¹*Metalurgy of the Rare Metals 7: Beryllium*, edited by G. E. Darwin and J. H. Buddery (Butterworths, London, 1960).
- ²²F. D. Feiock and W. R. Johnson, *Phys. Rev.* 187, 39 (1969).
- ²³R. P. Gupta and S. K. Sen, *Phys. Rev. A* 8, 1169 (1973).
- ²⁴R. Vianden, *Hyp. Interact.* 2, 169 (1976).
- ²⁵D. Quitmann, K. Nishiyama, and D. Riegel, in *Magnetic Resonance and Related Phenomena*, edited by P. S. Allen, E. R. Andrew, and C. A. Bates (North-Holland, Amsterdam, 1975), p. 349.
- ²⁶P. Jena, *Phys. Rev. Lett.* 36, 418 (1976).